

Properties of monovacancies and self-interstitials in bcc Na: An *ab initio* pseudopotential study

U. Breier, W. Frank, C. Elsässer, M. Fähnle, and A. Seeger

*Max-Planck-Institut für Metallforschung, Institut für Physik and Universität Stuttgart,
Institut für Theoretische und Angewandte Physik, D-70569 Stuttgart, Federal Republic of Germany*

(Received 5 April 1994)

By means of *ab initio* pseudopotential theory and the local-density approximation various properties of monovacancies and self-interstitials in bcc Na, viz. the formation energies and formation volumes and the electric field gradients in the neighborhood of the defects, are calculated. As in the case of Li treated earlier, comparison with experimental results leads to the following conclusions. (i) An interstitialcy mechanism of self-diffusion may be excluded. (ii) The vacancy formation enthalpy is so close to the activation enthalpy of self-diffusion that either the vacancy migration enthalpy must be extraordinarily small (this raises the question of the validity of the transition state theory) or the low-temperature self-diffusion in Na is due to a direct exchange of neighboring atoms or to a ring mechanism involving three atoms. A nonvacancy mechanism is supported by the fact that the calculated monovacancy formation volume at 0.51 atomic volumes is substantially larger than the experimentally determined activation volume of the low-temperature mechanism of self-diffusion.

I. INTRODUCTION

The simplest intrinsic defects we might have in a metal are vacancies and self-interstitials. A monovacancy is generated by removing an atom from a lattice site and inserting it at a typical surface site. The enthalpy difference between the final and the initial states of this process is the monovacancy formation enthalpy, H_{1V}^F . A self-interstitial is generated by removing an atom from a typical surface site and inserting it into an interstice in the interior of the crystal. The enthalpy of self-interstitial formation, H_I^F , is obtained in analogy to H_{1V}^F , but here we have to keep in mind that even in metals with simple crystal structures several mechanically stable self-interstitial configurations may exist with different formation enthalpies.

The migration of vacancies through a crystal leads to self-diffusion. This is true also for the migration of self-interstitials if it occurs, as is the rule, by an interstitialcy mechanism, i.e., by the exchange of an atom in an interstice with a neighboring one located (approximately) at a lattice site. In thermal equilibrium usually several mechanisms contribute to the self-diffusivity D^{SD} . If we denote the contribution of a given mechanism by D_j^{SD} , the corresponding self-diffusion activation enthalpy is defined as

$$H_j^{SD} := - \left. \frac{\partial \ln D_j}{\partial (1/k_B T)} \right|_{p=\text{const}}, \quad (1)$$

where k_B denotes Boltzmann's constant, T the absolute temperature, and p the hydrostatic pressure. For mechanisms involving lattice defects, H_j^{SD} is related to the enthalpies of formation and migration of the j defects, H_j^F and H_j^M , by

$$H_j^{SD} = H_j^F + H_j^M. \quad (2)$$

If we leave aside the possibility of short-circuit diffusion along extended defects, thermal-equilibrium self-diffusion at sufficiently low temperatures is dominated by the mechanism with the lowest H_j^{SD} . Owing to the experimental progress of the last few years, for many metals this value can be determined with an accuracy of the order of magnitude of 1%. If we succeed in identifying the underlying mechanism, Eq. (2) may give us important quantitative information on the defects involved. Note that in general the quantities on the right-hand side of (2) are much more difficult to determine from experiment than the left-hand side. Moreover, in some metals the assignment of measured migration enthalpies to intrinsic defects is controversial.

Among the measurements that have proved helpful in identifying mechanisms of self-diffusion are the dependences of the self-diffusivity on the atomic mass, characterized by the so-called isotope effect parameter

$$E^{\alpha,\beta} := \frac{(D^\alpha/D^\beta) - 1}{(m^\beta/m^\alpha)^{1/2} - 1}, \quad (3)$$

where D^α (D^β) denotes the diffusivity of the isotope with atomic mass m^α (m^β), and on the hydrostatic pressure, from which we may derive the self-diffusion volume

$$V_j^{SD} := -k_B T \left. \frac{\partial \ln D_j^{SD}}{\partial p} \right|_{T=\text{const}}. \quad (4)$$

Application of criteria which allow us to exclude certain mechanisms of self-diffusion confirmed the general belief that the dominant mechanism of self-diffusion in metals is the monovacancy mechanism for all face-centered-cubic (fcc) and all hexagonal close-packed metals on which de-

tailed experimental data are available but not for the body-centered-cubic (bcc) metals.¹ Among the bcc metals there is only one, viz., α -Fe, for which the dominance of the monovacancy mechanism could be established definitely. For two bcc metals, viz., Li and Na, the analysis of the experimental results has led to serious doubts whether any defect mechanism can account for the low-temperature self-diffusion data.¹ If these doubts are confirmed, the only remaining mechanisms are those involving the exchange of adjacent atoms without participation of lattice defects. It has been shown that such mechanisms are compatible with the experimental data available on Li (Refs. 1 and 2) and Na.¹

Under the circumstances just described, calculations of H_j^F and H_j^M (which for $p = 0$ coincide with the energies of formation and migration, E_j^F and E_j^M) on Li and Na might provide help in clarifying the situation. The inspection of existing calculations is not too encouraging, however. The results obtained by empirical or semiempirical calculations depend very sensitively on the values of the fit parameters. E.g., values for the monovacancy formation energy³ E_{1V}^F of bcc Na calculated in this way scatter between 0.42 eV (Ref. 4) and 0.15 eV.⁵ The difference between these two values is highly significant in the present context, as may be seen as follows. If the first value (obtained with empirical pseudopotentials) was (approximately) correct, we could exclude the vacancy mechanism of self-diffusion since then the measured activation enthalpy for the self-diffusion mechanism dominating at low temperatures, $H^{SD} = 0.37$ eV,^{6,7} would be incompatible with (2). The second value (obtained with interatomic pair potentials), however, leaves enough room to accommodate a positive vacancy migration enthalpy in (2).

The preceding examples indicate that empirical or semiempirical calculations are unlikely to be helpful in the present context and that it is only from *ab initio* calculations that we can hope to obtain quantitative theoretical information that can be relied upon. Recently, it has indeed been demonstrated that *ab initio* calculations based on the local-density approximation (LDA) are capable of giving a value for E_{1V}^F in Al with an accuracy which matches or possibly even exceeds that of the experimental determinations.^{8,9} LDA calculations on bcc Li based on *ab initio* pseudopotential theory¹⁰ gave the result that the formation energies E_I^F of all conceivable self-interstitial configurations are at least 40% larger than the experimentally observed^{2,11} low-temperature activation enthalpy for self-diffusion, $H^{SD} = (0.52 \pm 0.02)$ eV, whereas the calculated value $E_{1V}^F = 0.54$ eV coincides with H^{SD} within the combined errors of experiment and theory. Since in order to be physically meaningful, defect migration energies must be positive and at least a few times $k_B T$, the results of the LDA *ab initio* calculations on Li support the conjecture¹ that the dominant mechanism of self-diffusion in bcc Li is neither a self-interstitial nor a vacancy mechanism. The conclusion¹ that the dominant self-diffusion mechanism must then be a nondefect mechanism involving e.g., the direct exchange between nearest-neighbor atoms or a so-called ring mechanism¹² will be tested by *ab initio* calculations

of the saddle-point energies for vacancy migration and for the direct exchange of neighboring atoms in bcc Li (cf. Sec. IV B).

As mentioned above, the experimental situation with respect to the mechanism of self-diffusion in bcc Na is similar to that in Li, although the detailed reasoning is different due to the fact that the available experimental information is not the same. It appeared therefore appropriate to perform *ab initio* pseudopotential calculations in the local-density approximation on bcc Na, too, in order to check whether a similar situation arises as for bcc Li. The present paper considers monovacancies as well as various self-interstitial configurations, viz., octahedral and tetrahedral interstitials and the so-called $\langle 100 \rangle$, $\langle 110 \rangle$, and $\langle 111 \rangle$ dumbbells. The general guidelines in setting up the computations are outlined elsewhere.⁹

II. CONSTRUCTION OF THE PSEUDOPOTENTIAL AND THE COHESIVE PROPERTIES OF bcc Na

The frozen-core pseudopotential was constructed according to Hamann, Schlüter, and Chiang¹³ with a reference configuration (Ne) $3s^{0.7} 3p^{0.15} 3d^{0.15}$ and $r_{c,s} = r_{c,p} = 1.5$ a.u., $r_{c,d} = 1.8$ a.u. The cutoff radius r_{PC} for the partial-core correction¹⁴ was chosen in such a way that for $r = r_{PC}$ the core charge density was equal to the valence charge density; the cutoff radius q_{\max} for the pseudopotential in Fourier space was 7.9 (a.u.)⁻¹. The transferability of the pseudopotential was tested for several excited states. The excitation energies computed with the pseudopotential agreed with the all-electron results within 10^{-4} Ry.

The cubic lattice parameter a_0 and the bulk modulus K of the perfect lattice as obtained by converging the results with respect to the plane-wave energy cutoff E_c and the number n_1 of k points in the irreducible part of the Brillouin zone are given in Table I. The comparison of the present results with those of augmented-plane-wave (APW) calculations and full-potential linear-augmented-plane-wave (FLAPW) calculations of Sigalas *et al.*¹⁵ shows excellent agreement with the FLAPW calculations (see Table I). In agreement with the general experience with LDA calculations, all three computational

TABLE I. Calculated equilibrium lattice parameter a_0 and elastic bulk modulus K of bcc Na, in comparison with other theoretical and with experimental data. The experimental value of K was obtained at 78 K, that of a_0 at 5 K.

| | a_0 [10^{-10} m] | K [GPa] |
|--------------------|-----------------------|------------------|
| This paper | 4.05 | 9.12 |
| FLAPW ^a | 4.05 | 9.2 |
| APW ^a | 4.07 | 8.7 |
| Experiment | 4.225 ^b | 7.3 ^c |

^aReference 15.

^bReference 16.

^cReference 17.

methods overestimate the bulk modulus and slightly underestimate the lattice parameter.

III. PROPERTIES OF MONOVACANCIES AND SELF-INTERSTITIALS

A. Definitions and some computational details

The present computations of defect properties in Na use periodic arrangements of supercells with either 16 or 54 atoms in the defect-free cells. The defects are inserted in the supercell centers. Since in this approach there are no surfaces, the recipe of Sec. I for the calculation of the formation energies of interstitials and vacancies cannot be followed. Instead, the formation energies are calculated according to

$$E_I^F = E(N + 1, 1, \Omega_I) - \frac{N + 1}{N} E(N, 0, N\Omega_0) \quad (5)$$

or

$$E_{1V}^F = E(N - 1, 1, \Omega_{1V}) - \frac{N - 1}{N} E(N, 0, N\Omega_0) \quad (6)$$

Here $E(N \pm 1, 1, \Omega_j)$ denotes the energy of a supercell with $N \pm 1$ atoms and either one self-interstitial or one vacancy at the respective equilibrium volume Ω_j , and $E(N, 0, N\Omega_0)$ the energy of an ideal supercell with N atoms at the equilibrium volume $N\Omega_0$. The relaxation of the atomic positions around the defects is performed by first moving the atoms according to the Hellmann-Feynman forces until the forces acting on the atoms are zero (“structural relaxation”). During this first step the supercell volume is kept constant; i.e., $\Omega_j = N\Omega_0$ is maintained. In a second step the system is allowed to shrink or expand homogeneously (“volume relaxation”) until the total energy reaches its minimum. The handling of numerical problems encountered in the second step is described elsewhere.¹⁸ For a vacancy in Li, the forces on the atoms were calculated again after this second relaxation step.¹⁸ Since it turned out that these forces were very small and that the corresponding relaxation of the atomic positions had virtually no effect on the formation energy, in the present work we have refrained from recalculating the forces after the volume relaxation.

The formation volume

$$V_j^F := -\partial G_j^F / \partial p|_{T=\text{const}} \quad (7)$$

of the j defects is defined in terms of the pressure dependence of their free enthalpy of formation (Gibbs free energy), G_j^F , which at $T = 0$ reduces to H_j^F . The self-diffusion volume V_j^{SD} [defined by Eq. (4)] is related to V_j^F and is, as experience shows, numerically not too different from it. Comparison of calculated V_j^F volumes with measured self-diffusion volumes can therefore give an important hint of the diffusion mechanism.

From the procedure of generating a vacancy or a self-interstitial as described in Sec. I it follows that the va-

cancy formation volume is given by

$$V_{1V}^F = \Omega_0 + \Delta V_{1V} \quad (8)$$

and the self-interstitial formation volume by

$$V_I^F = -\Omega_0 + \Delta V_I \quad (9)$$

where ΔV_j ($j = 1V, I$) denotes the change of the volume of a large crystal with traction-free surfaces per j -type defect introduced. For both vacancies and self-interstitials the quantity ΔV_j may be determined from a supercell calculation according to^{19,20}

$$\Delta V_j = \Omega_j - N\Omega_0 \quad (10)$$

The quantities Ω_j , already introduced in Eqs. (5) and (6), are the volumes of the supercells into which one vacancy or one self-interstitial has been introduced and on which the complete relaxation procedure described above has been carried out. ΔV_j is to be distinguished from the local relaxation volume ΔV_j^∞ , which does not include the volume change that results from the “image defects” that one requires in order to have traction-free surfaces of a finite crystal and which is therefore a better measure of the local relaxation around a defect than ΔV_j . The two quantities are related to each other by

$$\Delta V_j = \Delta V_j^\infty (1 + \gamma) \quad (11)$$

where $\gamma > 0$ is the so-called Eshelby factor.²¹ The Eshelby factor may be calculated from the elastic constants. Its numerical values are $\gamma = 0.37$ for Na and $\gamma = 0.40$ for Li.²²

B. Relaxation displacements of atoms

Figure 1 shows the differences between the distances d of the individual atoms from the supercell center as obtained after the first relaxation step (i.e., without volume relaxation) and the distances d_0 in the perfect crystal. It should be noted that for atoms on the supercell boundary, symmetry restrictions force components of the displacement vector to be zero (see caption of Fig. 1). The relaxation around the vacancy looks very much like that obtained for Li.^{10,18,23} The introduction of a dumbbell at the center of the supercell breaks the cubic symmetry of the ideal lattice. As a result, atoms which originally had the same distance from the center of the unit cell may experience different displacements when a dumbbell is introduced, as shown in Fig. 1 for a $\langle 100 \rangle$ dumbbell. The separation of the dumbbell atoms after the structural relaxation is 5.31 a.u., 5.51 a.u., and 5.47 a.u. for the $\langle 100 \rangle$, $\langle 110 \rangle$, and $\langle 111 \rangle$ dumbbells, respectively.

C. Vacancy formation energy and formation volume

Table II gives the results for the vacancy formation energy as calculated without relaxation (n.r.) and after the first relaxation step (w.r.) for $N = 16, 54$, and for vari-

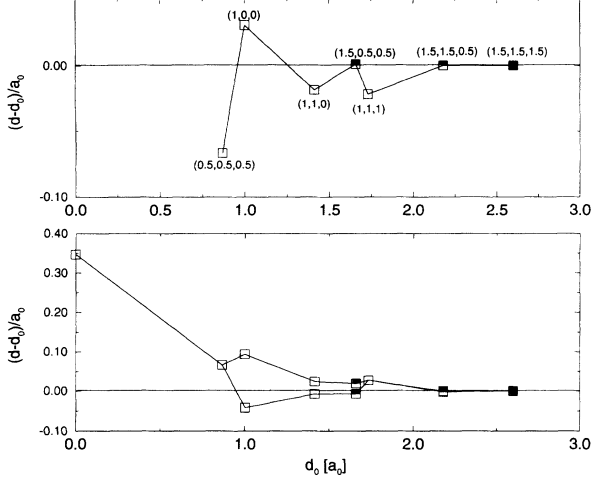


FIG. 1. Displacement of the neighboring atoms around the vacancy (top) and the $\langle 100 \rangle$ dumbbell (bottom). The figure shows the modification of the distance d in the defect center as a function of the original distance d_0 , in units of the original lattice constant a_0 . The lines are guidelines for the eyes. There is no displacement of the outermost atom due to the periodicity of the superlattice. For the $\langle 100 \rangle$ dumbbell we present for $d_0 = 0$ the distance of the dumbbell atoms from the center of the supercell, i.e., half the separation of the dumbbell atoms. Atoms denoted by the symbol \blacksquare (■) are located on a supercell boundary and hence one (all) components of their displacement vector are forced to be zero due to symmetry restrictions.

ous values of E_c and numbers n of k points used in the Brillouin-zone sampling. In order to facilitate the comparison of the convergence with respect to the Brillouin-zone sampling for various supercell sizes, we also exhibit the number n_1 of k points which had to be used in a one-atom supercell in order to get the same single-particle states as in a perfect 16- or 54-atom supercell (“equivalent set”). The convergence of the data for $N = 54$ with

TABLE II. Vacancy formation energy E_{1V}^F as calculated for different numbers N of sites in the supercell, different cutoff energies E_c of the plane-wave basis, and different numbers n of k points in the irreducible Brillouin zone of the superlattice. The corresponding numbers n_1 of k points in the irreducible Brillouin zone of a one-atom unit cell are also given. The superscripts a and b denote high-symmetry and low-symmetry k points, respectively (1 Ry = 13.6058 eV).

| N | E_c [Ry] | k points | | E_{1V}^F [eV] | |
|-----|------------|----------------|-------|-----------------|------|
| | | n | n_1 | n.r. | w.r. |
| 16 | 8.5 | 4 | 14 | 0.55 | |
| | 8.5 | 4 | 40 | | 0.40 |
| | 8.5 | 10 | 112 | 0.44 | 0.40 |
| | 8.5 | 20 | 240 | | 0.40 |
| | 10.5 | 1 | 5 | -0.21 | |
| 54 | 10.5 | 4 | 14 | 0.55 | |
| | 8.5 | 1 | 8 | | 0.47 |
| | 8.5 | 4 ^a | 30 | 0.45 | 0.40 |
| | 8.5 | 4 ^b | 112 | | 0.36 |

respect to n_1 resembles very much that found in Li:¹⁰ E_{1V}^F decreases by 0.11 eV when going from $n_1 = 8$ to $n_1 = 112$. In earlier calculations on Li the step from $n_1 = 112$ to $n_1 = 728$ had virtually no effect. Analogously, we found for Na ($N = 54$, $E_c = 8$ Ry) a change of only 0.006 eV when going from $n_1 = 112$ to $n_1 = 330$. The comparison of the results for $N = 16$, $n_1 = 14$, and $E_c = 8.5$ Ry or 10.5 Ry shows that the E_{1V}^F values are already very close to convergence at $E_c = 8.5$ Ry, again as was the case in Li.¹⁰ (The reason for this is that E_{1V}^F , representing the *difference* between two total energies, converges much more rapidly than the individual total energies.) We therefore suppose that our results for $N = 16$ and $N = 54$ are very close to convergence already at $E_c = 8.5$ Ry and $n_1 = 112$.

Concerning the convergence with respect to the supercell size, it has recently been shown¹⁹ that for cubic crystals that part of the vacancy formation energy which depends on the supercell size N originates almost exclusively from elastic interactions between the vacancies. Correcting for these elastic interactions, we arrive at an extrapolated value of $E_{1V}^F = 0.340$ eV for an isolated vacancy in Na. The uncertainty of this value due to the limitation of the LDA is difficult to estimate from theory, but the comparison between experiment and theory on Al (Refs. 8 and 9) referred to in Sec. I leads us to believe that the uncertainty resulting from this does not exceed 5%.

Finally we have to discuss the effect of the second relaxation step, the so-called volume relaxation, on E_{1V}^F . This step involves finding that supercell volume at which the energy of a supercell containing a vacancy is lowest. It turns out that the dependence of E_{1V}^F on the relaxation volume is rather weak. This has the advantageous consequence that the volume relaxation has a very small effect on E_{1V}^F . E.g., the vacancy formation energy as obtained from a supercell with $N = 54$ was reduced by only 4 meV. We thus obtain as our final result

$$E_{1V}^F(\text{Na}) = (0.34 \pm 0.02) \text{ eV} \quad (12)$$

On the other hand, the weak dependence of E_{1V}^F on Ω_{1V} has the consequence that the accurate determination of the vacancy formation volume requires extensive and careful numerical work. The supercell volume Ω_{1V} was determined by the second relaxation step described in Sec. III A for $N = 54$, $E_c = 8.5$ Ry, and $n_1 = 112$. Since the Ω_{1V} obtained in this way could not be expected to be close to convergence with respect to E_c and n_1 , we calculated ΔV_{1V} by inserting into Eq. (10) the perfect-lattice value Ω_0 following from a one-atom-unit-cell calculation using the same E_c and an equivalent set of k points. In this way we found from Eq. (10)

$$\Delta V_{1V} = -0.49\Omega_0, \quad (13)$$

which is close to the result $\Delta V_{1V} = -0.51\Omega_0$ obtained for Li.¹⁰

The preceding procedure was based on the assumption that the errors in Ω_{1V} and $N\Omega_0$ due to the incomplete convergence tend to cancel in the determination of ΔV_{1V} from Eq. (10) (cf. the analogous reasoning in the calculation of the formation energy given above). The validity of

this assumption was tested by computations on a supercell with $N = 16$. The calculations with $E_c = 8.5$ Ry and a set of k points equivalent to that used for the $N = 54$ calculations gave us $\Delta V_{1V} = -0.45\Omega_0$. Going to $E_c = 10.5$ Ry but keeping the number of k points constant led to $\Delta V_{1V} = -0.46\Omega_0$, i.e., to a rather small change. We take these results as evidence that the value (13) obtained for a supercell with $N = 54$ is indeed close to convergence with regard to E_c and n_1 . We have also determined ΔV_{1V} from the pressure generated by forming a vacancy at constant volume,¹⁸ yielding again the result (13). Insertion of (13) into (8) gives us as the calculated value of the monovacancy formation volume of bcc Na

$$V_{1V}^F = 0.51\Omega_0 \quad (14)$$

From (14) and the Eshelby factor for Na follows the local relaxation volume as $\Delta V_{1V}^\infty = -0.36\Omega_0$. Nearly the same value was found in the computations on Li.¹⁰

D. Formation energies and formation volumes for self-interstitials

Tables III and IV give the formation energies E_I^F of the various self-interstitial configurations as calculated without taking into account the volume relaxation. Table III shows the data for the unrelaxed $N = 16$ supercell with $E_c = 8.5$ Ry and $n_1 = 14$. Because E_I^F is much higher for the octahedral and the tetrahedral interstitials than for the dumbbell configurations, we have performed the $N = 54$ supercell calculations only for the dumbbells. From Table IV it becomes obvious that the *structural* relaxation affects their formation energies much more than the vacancy formation energy. As in the case of Li, even the lowest self-interstitial formation energies, those of $\langle 110 \rangle$ and $\langle 111 \rangle$ dumbbells, exceed the vacancy formation energy considerably.

Because the influence of the volume relaxation was expected to be larger for self-interstitials than for vacancies, we have estimated the order of magnitude of the reduction of E_I^F by calculations on the $\langle 110 \rangle$ dumbbell in a $N = 54$ supercell for cell volumes Ω_I that had been increased by one and two atomic volumes (for 30 k points in the irreducible Brillouin zone; see Table IV). In both cases the formation energy 0.59 eV obtained with the cell volume $N\Omega_0$ was reduced by 0.039 eV. From this result we conclude that the equilibrium volume lies between

TABLE III. Results for the formation energies E_I^F of various self-interstitial configurations for a $N = 16$ supercell without relaxation ($E_c = 8.5$ Ry, $n_1 = 14$).

| Configuration | E_I^F [eV] |
|--------------------------------|--------------|
| Octahedral site | 2.67 |
| Tetrahedral site | 3.88 |
| $\langle 111 \rangle$ dumbbell | 1.37 |
| $\langle 110 \rangle$ dumbbell | 1.65 |
| $\langle 100 \rangle$ dumbbell | 1.21 |

TABLE IV. Results for the formation energies of various self-interstitial configurations for a $N = 54$ supercell without relaxation (n.r.) and with relaxation (w.r.), $E_c = 8.5$ Ry. The superscripts a and b denote high-symmetry and low-symmetry k points, respectively.

| k points | | E_I^F [eV] | | | | | |
|----------------|-------|-----------------------|------|-----------------------|------|-----------------------|------|
| n | n_1 | $\langle 111 \rangle$ | | $\langle 110 \rangle$ | | $\langle 100 \rangle$ | |
| | | n.r. | w.r. | n.r. | w.r. | n.r. | w.r. |
| 1 | 8 | | 0.97 | | 0.99 | | 1.10 |
| 4 ^a | 30 | 1.99 | 0.60 | 1.70 | 0.59 | 1.46 | 0.73 |
| 4 ^b | 112 | | 0.64 | | | | |

$(N + 1)\Omega_0$ and $(N + 2)\Omega_0$ and that the influence of the volume relaxation on the formation energy of the self-interstitial exceeds that on E_{1V}^F but is nevertheless not large enough to reduce E_I^F to values comparable with the vacancy formation energy.

Since on the basis of the computed formation energies we can rule out the possibility of a significant interstitial contribution to self-diffusion in Na, there was no great interest in determining ΔV_I accurately. From the calculation of E_I^F for $\langle 110 \rangle$ dumbbells at prescribed values $\Delta V_I = 0, \Omega_0$, and $2\Omega_0$ (see above) we may conclude that V_I^F is positive but not larger than one atomic volume.

E. Electric field gradients

The lattice sites in bcc and fcc crystals have cubic point symmetry. Hence the electric field gradients at these sites are zero. The introduction of defects, e.g., of vacancies or self-interstitials, destroys the symmetry at neighboring sites. As a consequence, electric field gradients act on the nuclei of neighboring atoms. If these nuclei possess sufficiently large nuclear quadrupole moments Q , as ²³Na with ²⁴ $Q = (109 \pm 3) \times 10^{-31} \text{ m}^2$ does, those electric field gradients may be investigated by nuclear magnetic resonance (NMR) techniques. If we adopt for the principal components of the (traceless) tensor \mathbf{V} of the electric field gradient (EFG) the convention $|V_{zz}| \geq |V_{yy}| \geq |V_{xx}|$, the so-called asymmetry parameter

$$\eta = \frac{V_{yy} - V_{xx}}{V_{zz}} \quad (15)$$

obeys $0 \leq \eta \leq 1$. For a nucleus such as ²³Na with spin $I = 3/2$ each electric field gradient gives rise to a quadrupolar resonance frequency

$$\nu_Q = \frac{eQ}{2} |V_{zz}| \left(1 + \frac{\eta^2}{3} \right)^{1/2}, \quad (16)$$

where e is the elementary charge. Since V_{zz} and η at the nuclei in the various shells around the defects are different, the set of quadrupolar resonance frequencies associated with a given defect constitutes a “fingerprint” of that defect. Calculations of V_{zz} and η are therefore of considerable interest.

Admittedly, the present pseudopotential calculation is not the most suitable method to obtain accurate numerical results for the electric field gradients. First, the frozen-core approximation neglects the contribution arising from the polarization of the ionic cores in the inhomogeneous potential fields. However, for the electric field gradient acting on the nuclei in ideal hexagonal metals, these core polarization effects play only a minor role.²⁵ To which extent this is also true for nuclei close to atomic defects has not yet been investigated. Second, the valence contribution to the electric field gradient is not correctly represented by the pseudo-wave-function, since it may exhibit the correct asphericity but not the correct radial dependence, which also affects the electric field gradient. In spite of these shortcomings we think that the general behavior and the order of magnitude of our results on the EFG are correct. (See, however, note added in proof.)

Table V summarizes the results for the vacancy and the $\langle 100 \rangle$ dumbbell in Na. The general features resemble very much those of Li.²⁶ Some of these presumably apply to other metals, too. E.g., the result that in Li and Na the electric field gradients at the next-nearest neighbors of a vacancy are considerably larger than those at the nearest neighbors and that hence the sites with the largest value of $|V_{zz}|$ are not necessarily those closest to the defect may hold for other bcc metals as well. Another result that is likely to be of general validity is that the largest values of $|V_{zz}|$ associated with dumbbell self-interstitials (which appear to occur always at the sites of the dumbbell atoms, i.e., in the $m = 0$ shell) are much larger than the largest $|V_{zz}|$ associated with vacancies in the same metal. This result, which is supported by re-

TABLE V. The frequencies ν_Q of the quadrupolar splitting at nuclei close to a vacancy and to a $\langle 100 \rangle$ dumbbell. The integer m denote the shells around the defect center where the considered atom is located in the unrelaxed supercell ($m = 0$ corresponds to the dumbbell atoms). Note the symmetry breaking due to relaxation after the introduction of the dumbbell for $m = 2, 3, 4, 6$. The quantity N_m denotes the number of atoms in the corresponding crystallographically equivalent positions. For atoms at the supercell boundary the results are strongly influenced by the supercell geometry. E.g., the large value of η for $m = 4$ arises from the fact that these atoms lie on the supercell boundary.

| Shell m | Vacancy | | | $\langle 100 \rangle$ dumbbell | | |
|--------------|---------|-----------------------------------|--------|--------------------------------|-----------------------------------|--------|
| | N_m | ν_Q [10^3 s^{-1}] | η | N_m | ν_Q [10^3 s^{-1}] | η |
| 0 | 0 | — | — | 2 | 66.1 | 0.00 |
| 1 | 8 | 5.4 | 0.00 | 8 | 13.7 | 0.17 |
| 2 | 6 | 9.7 | 0.00 | 4 | 2.8 | 0.08 |
| | 0 | | | 2 | 38.5 | 0.00 |
| 3 | 12 | 3.7 | 0.03 | 8 | 4.3 | 0.01 |
| | 0 | | | 4 | 3.6 | 0.75 |
| 4 | 24 | 4.1 | 0.97 | 16 | 4.7 | 0.98 |
| | 0 | | | 8 | 3.9 | 0.92 |
| 5 | 8 | 2.0 | 0.00 | 8 | 7.1 | 0.35 |
| 6 | 24 | 4.3 | 0.00 | 8 | 4.2 | 0.79 |
| | 0 | | | 16 | 4.3 | 0.00 |
| 7 | 8 | 0 | 0.00 | 8 | 3.2 | 0.00 |

cent experiments on irradiated and quenched copper,^{27,28} is clearly very helpful in assigning the EFG “fingerprints” to definite defects.

IV. DISCUSSION

A. Enthalpies of formation

One important result of the present computations is that in Na the enthalpy of formation of self-interstitials is by about a factor 1.8 larger than that of monovacancies, which means that we may disregard the contributions of self-interstitials to the defects in thermal equilibrium. We are thus justified in interpreting the high-temperature measurements of the relative change of the lattice parameter, $\Delta a_0/a_0$, and of the specimen’s length, $\Delta l/l$, in terms of

$$C_V^{\text{eq}} = \frac{1}{3} \left[\frac{\Delta l}{l} - \frac{\Delta a_0}{a_0} \right], \quad (17)$$

where C_V^{eq} is the total atomic concentration of vacancies in thermal equilibrium.²⁹ Feder and Charbneau³⁰ carried out such measurements on Na and found, by fitting their results to

$$C_V^{\text{eq}}(T) = \exp\left(\frac{S_{\text{eff}}^F}{k_B}\right) \exp\left(-\frac{H_{\text{eff}}^F}{k_B T}\right), \quad (18)$$

an effective formation enthalpy $H_{\text{eff}}^F = (0.42 \pm 0.03) \text{ eV}$ and an effective formation entropy $S_{\text{eff}}^F = (5.8 \pm 1.1)k_B$. By combining the x-ray determinations of $\Delta a_0/a_0$ of Feder and Charbneau³⁰ with their own $\Delta l/l$ data as obtained by means of a capillary method, Ritter *et al.*³¹ derived $H_{\text{eff}}^F = (0.40 \pm 0.05) \text{ eV}$ and $S_{\text{eff}}^F = (7.2 \pm 1.5)k_B$. Adhart *et al.*³² determined $\Delta a_0/a_0$ by neutron scattering. Combining these data with the $\Delta l/l$ measurements of Feder and Charbneau³⁰ gave them $H_{\text{eff}}^F = (0.354 \pm 0.025) \text{ eV}$, $S_{\text{eff}}^F = (3.9 \pm 0.7)k_B$, whereas combining them with those of Ritter *et al.*³¹ gave $H_{\text{eff}}^F = (0.36 \pm 0.03) \text{ eV}$, $S_{\text{eff}}^F = (4.0 \pm 0.9)k_B$. From specific heat measurements at high temperatures Martin³³ found $H_{\text{eff}}^F = (0.35 \pm 0.05) \text{ eV}$ and $S_{\text{eff}}^F = (5.2 \pm 1.3)k_B$.

Since at the beginning of this section a significant contribution of self-interstitials to the thermal-equilibrium population of intrinsic atomic defects in Na has been excluded, the differences between the effective enthalpy of formation, H_{eff}^F , and the monovacancy formation enthalpy H_{1V}^F (which for atmospheric pressure is numerically indistinguishable from E_{1V}^F , the quantity calculated in Sec. III C) must mainly come from divacancy contributions. As the formation enthalpy of divacancies exceeds that of monovacancies, the ratio of divacancies and single vacancies in thermal equilibrium increases with increasing temperature. A direct consequence of this is the inequality

$$H_{1V}^F < H_{\text{eff}}^F. \quad (19)$$

Equation (19) is indeed compatible with the calculated value (12) and the various experimental data discussed

in the preceding paragraph. The scatter in H_{eff}^F is too large to allow a quantitative estimate of the divacancy contribution to C_V^{eq} .

B. Self-diffusion

In Na the Arrhenius plot $\ln D^{\text{SD}}(T)$ vs $(k_B T)^{-1}$ is strongly curved.⁶ Together with the temperature dependences of the activation volume of self-diffusion [cf. Eq. (4)] and of the isotope energy parameter [cf. Eq. (3)], this indicates strongly that in Na several mechanisms with different enthalpies of self-diffusion, H_j^{SD} , contribute to self-diffusion. The key problem is to identify the mechanism that has the lowest activation enthalpy, which will be denoted by H_1^{SD} . It should be noted that the curvature of the Arrhenius plot was tentatively ascribed to a temperature dependence of the defect parameters rather than to the appearance of several mechanisms by Jacucci and Taylor.³⁴ The discussion of such a probable temperature dependence is not relevant for the present paper, where we consider exclusively the low-temperature limit of the effective enthalpy of self-diffusion obtained by extrapolation of the experimental data (see below).

At low enough temperatures the effective enthalpy of bulk self-diffusion, $H_{\text{eff}}^{\text{SD}}$, should approach H_1^{SD} . The measurements on Na do not extend to sufficiently low temperatures for $H_{\text{eff}}^{\text{SD}}$ to become temperature independent; H_1^{SD} must therefore be found by extrapolation. By fitting his ²²Na tracer data, which extend down to a self-diffusivity of about 10^{-16} m²/s, to the superposition of two Arrhenius laws, Mundy⁶ obtained $H_1^{\text{SD}} = 0.37$ eV. The same value was derived from an analogous fit to the dipolar contribution to the ²³Na spin-lattice relaxation time.³⁵ If we assume that H_1^{SD} is to be attributed to monovacancies and that hence Eq. (2) holds, we arrive at the conclusion that in Na the monovacancy migration enthalpy is only about 0.03 eV. This is such a small value (note that 0.02 eV = $230k_B$ K) that the validity of the physical picture leading to Eq. (2) cannot be taken for granted. Alternatively, we may argue that the monovacancy migration enthalpy is large enough for Eq. (2) to be valid, say, larger than $3k_B T \approx 0.06$ eV. We then have to conclude that the monovacancy mechanism cannot be responsible for the low-temperature bulk self-diffusion of bcc Na. Since interstitialcy and multiple-vacancy mechanisms for self-diffusion may be excluded *a fortiori*, the only remaining possibilities are nondefect mechanisms, e.g., the direct exchange of neighboring atoms or a ring mechanism.¹² It remains to be seen whether further calculations will be able to demonstrate that a nondefect mechanism can give H_1^{SD} values that are compatible with the experimental data.

Another way in which *ab initio* calculations may help to distinguish between the monovacancy mechanism and a nondefect mechanism of self-diffusion is to consider the activation volumes

$$V_{1V}^{\text{SD}} = -k_B T \left. \frac{\partial \ln D_{1V}^{\text{SD}}}{\partial p} \right|_{T=\text{const}} \quad (20)$$

of the monovacancy mechanism and

$$V_{\text{exch}}^{\text{SD}} = -k_B T \left. \frac{\partial \ln D_{\text{exch}}^{\text{SD}}}{\partial p} \right|_{T=\text{const}} \quad (21)$$

of a direct exchange mechanism. Analogous equations hold for ring mechanisms. In the first case we may write in analogy to Eq. (2)

$$V_{1V}^{\text{SD}} = V_{1V}^F + V_{1V}^M, \quad (22)$$

where V_{1V}^F is the vacancy formation volume. This quantity may be obtained experimentally by measuring the pressure dependence of C_{1V}^{eq} , or calculated as discussed in Sec. III. The so-called migration volume V_{1V}^M then may be obtained from Eq. (22) with V_{1V}^{SD} determined experimentally according to Eq. (20). We should realize, however, that Eqs. (20), (22) are little more than an operational definition of the migration volume V_{1V}^M , since at present we do not know how to calculate V_{1V}^M from first principles. An analogous situation obtains for $V_{\text{exch}}^{\text{SD}}$.

The main difficulty in calculating V_{1V}^M and $V_{\text{exch}}^{\text{SD}}$ is as follows. Both quantities are related to the energy barrier over which the system has to pass during a diffusion jump. Since the crystal can respond to the movement of a jumping atom not faster than with the speed of sound, the atomic relaxation during this movement is confined to a rather small neighborhood of the atom that passes over the energy barrier. The fact that during jump processes the relaxation is necessarily incomplete means that the true activation enthalpy is larger than the saddle-point energy as calculated by the present (or any other static) computational technique. In situations in which the relaxation has only a modest effect on the computed energies this violation of one of the basic assumptions of the so-called transition state theory of rate processes may be a small effect. It is indeed likely that the above comparison between H_1^{SD} and H_{1V}^F is valid to quite a good approximation. The situation is, however, completely different when we consider activation and migration volumes. We must expect substantial differences between the numerical values deduced from experiment by means of Eqs. (20)–(22) and those obtained from static treatments of saddle-point configurations. As in the case of the formation volume (Sec. III A) the volume changes obtained for the saddle-point configuration from static supercell calculations are identical to the ones found from static calculations for a finite sample with a traction-free surface. However, it is obvious that the image forces that are necessary to keep the surface of a large but finite sample stress free cannot respond to the movements during a jump. This means that the measured values of $|V_{1V}^M|$ or $|V_{\text{exch}}^{\text{SD}}|$ cannot exceed the so-called “local volumes,” which are the static values divided by $(1 + \gamma)$, where γ is the Eshelby factor (see Sec. III A). However, even these values will be too large since during the jump the relaxation is confined to the close neighborhood of the jumping atom.

The preceding considerations find experimental support on the one hand in the measurements of the pressure dependence of the diffusivity of foreign atoms such as C, N, and O interstitially dissolved in metals, and on the

other hand in all those cases where both V_{1V}^{SD} and V_{1V}^F have been determined experimentally. The experiments on N and O in vanadium, on N and C in α -Fe, and on C in Ni and α -Co have all given migration volumes that are small compared with the atomic volume (in some case, e.g., C in Ni, they were even negative).³⁶ On all metals on which there is experimental information on both V_{1V}^{SD} and V_{1V}^F , the difference $|V_{1V}^{SD} - V_{1V}^F|$ was found to be much smaller than V_{1V}^{SD} .

The two-mechanism fit to the tracer self-diffusion data of Na mentioned above gave for the activation volume of the low-temperature mechanism of self-diffusion $V_1^{SD} = 0.32\Omega_0$.³⁷ However, this involved considerable extrapolation since the highest pressure employed was only 0.95 GPa and the lowest temperature as high as 288 K. The more directly obtained value $V_1^{SD} = 0.18\Omega_0$ (Refs. 35, 38) following from recent ²³Na NMR measurements down to lower temperatures and to much higher pressures appears to be considerably more reliable. The V_1^{SD} values just mentioned are distinctly smaller than the calculated monovacancy formation volume V_{1V}^F [cf. Eq. (14)]. While we cannot exclude the possibility that $V_{1V}^F - V_{1V}^{SD} > 0$ (i.e., that — if the low-temperature diffusivity is determined by vacancies — the migration volume is negative), by the theoretical arguments given above $|V_{1V}^F - V_{1V}^{SD}|$ should be much smaller than V_{1V}^F or V_{1V}^{SD} , in conflict with the experimental data. On the other hand, an activation volume of the order of magnitude $0.2\Omega_0$ appears quite plausible for a direct-exchange or ring mechanism of self-diffusion.

Finally, we consider the isotope effect parameter $E^{\alpha,\beta}$ [cf. Eq. (3)]. It increases rapidly⁶ as the temperature is lowered from the melting point (this is a very strong indication that self-diffusion in solid Na involves more than one mechanism, in contrast to a recent viewpoint³⁹) and reaches the level 0.38 below room temperature. The deviation from the maximum value $E^{\alpha,\beta} = 1$ is determined by the so-called correlation factor and the number of atoms participating in the diffusion jumps in addition to the tracer atom. $E^{\alpha,\beta} = 0.38$ is very well compatible with strongly relaxed monovacancies as the vehicles of self-diffusion. It is also fully compatible with a direct exchange of neighboring atoms, for which the maximum value is $E^{\alpha,\beta} = 0.5$. For a ring mechanism involving

n atoms one expects $E^{\alpha,\beta} \approx n^{-1}$. Since at the lowest temperature investigated⁶ ($T = 248$ K) a second mechanism still gives a substantial contribution, the isotope effect measurements are presumably also compatible with a three-ring mechanism but not with ring mechanisms involving more atoms (as those discussed by Doan and Adda⁴⁰).

We may state that on the qualitative level of reasoning of the preceding paragraphs the pressure dependence of the self-diffusion of Na is in better agreement with a nondefect low-temperature mechanism than with a mechanism involving defects. How can *ab initio* calculations help to strengthen or refute this conclusion? It is clearly desirable to carry out dynamic calculations that avoid the question of the applicability of the transition state theory and, at the same time, give reliable values for the isotope effect parameter $E^{\alpha,\beta}$. Realistic *ab initio* computations of this kind are not inconceivable but presumably beyond the potential of present-day computations. As an intermediate step it appears rewarding to study possible saddle-point configurations of direct-exchange or three-ring mechanisms by static methods. The comparison with experiment could be based, e.g., on the criteria that for the self-diffusion mechanism realized in nature, the saddle-point energy should be close to but slightly lower than the experimentally determined H_1^{SD} and that the calculated volume expansion in the saddle-point configuration must be larger than the self-diffusion volume by at least the factor $(1 + \gamma)$.

Note added in proof: In the meantime, we have calculated the electric field gradients for atoms near a vacancy in Na by reconstructing the real valence wave functions from the pseudovalence wave functions (details are given elsewhere), and by the FLAPW method. The results of the two methods agree very well, but show that (in contrast to the behavior of Li) the pseudopotential values given in Table V are too small by typically an order of magnitude.

ACKNOWLEDGMENTS

The authors are indebted to R. Pawellek, C.-T. Chan, and K.-M. Ho for helpful discussions.

¹ A. Seeger, Defect and Diffusion Forum **95-98**, 147 (1993).

² A. Feinauer, (Dr. rer. nat.) thesis, University of Stuttgart, 1993.

³ Since in the discussion of diffusion of metals one considers not only monovacancies but also divacancies, we distinguish them by the subscripts 1V or 2V. For self-interstitials (subscript I) a corresponding distinction is not necessary in the present context.

⁴ P.S. Ho, Phys. Rev. B **3**, 4035 (1971).

⁵ R.C. Brown, J. Worster, N.H. March, R.C. Perrin, and R. Bullough, Philos. Mag. **23**, 555 (1971).

⁶ J.N. Mundy, Phys. Rev. B **3**, 2431 (1971).

⁷ G. Brüngrer, O. Kanert, and D. Wolf, Phys. Rev. B **22**, 4247 (1980).

⁸ J. Furthmüller and M. Finnis (unpublished).

⁹ A. Seeger and M. Fähnle, in *Computer Aided Innovation of New Materials II*, edited by M. Doyama, J. Kihara, M. Tanaka, and R. Yamamoto (Elsevier Science, New York, 1993), p. 439.

¹⁰ W. Frank, U. Breier, C. Elsässer, and M. Fähnle, Phys. Rev. B **48**, 7676 (1993).

¹¹ R. Messer, A. Seeger, and K. Zick, Z. Metallkd. **80**, 299 (1989).

¹² C. Zener, Acta Crystallogr. **3**, 346 (1950).

¹³ D.R. Hamann, M. Schlüter, and C. Chiang, Phys. Rev. Lett. **43**, 1494 (1979).

¹⁴ M.M. Dacorogna and M.L. Cohen, Phys. Rev. B **34**, 4996 (1986).

- ¹⁵ M. Sigalas, N.C. Bacalis, D.A. Papaconstantopoulos, M.J. Mehl, and A.C. Switendick, *Phys. Rev. B* **42**, 11637 (1990).
- ¹⁶ C.S. Barrett, *Acta Crystallogr.* **9**, 671 (1956).
- ¹⁷ M.E. Diederich and J. Trivisonno, *J. Phys. Chem. Solids* **27**, 637 (1966).
- ¹⁸ R. Pawellek, M. Fähnle, C. Elsässer, K.-M. Ho, and C.-T. Chan, *J. Phys. Condens. Matter* **3**, 2451 (1991).
- ¹⁹ J. Mayer, M. Fähnle, and A. Seeger (unpublished).
- ²⁰ J.R. Hardy, *J. Phys. Chem. Solids* **29**, 2009 (1968).
- ²¹ J.D. Eshelby, in *Solid State Physics*, edited by F. Seitz and D. Turnbull (Academic Press, New York, 1956), Vol. 3, p. 79.
- ²² G. Leibfried and N. Breuer, *Point Defects in Metals I: Introduction to the Theory*, Springer Tracts in Modern Physics, Vol. 81, (Springer, Berlin, 1978).
- ²³ R. Benedek, L.H. Yang, C. Woodward, and B.I. Min, *Phys. Rev. B* **45**, 2607 (1992).
- ²⁴ P. Pyykö and J. Li (unpublished).
- ²⁵ P. Blaha, K. Schwarz, and P.H. Dederichs, *Phys. Rev. B* **37**, 2792 (1988).
- ²⁶ R. Pawellek, Dr. rer. nat. thesis, University of Stuttgart, 1991.
- ²⁷ M. Notter, K. Konzelmann, G. Majer, and A. Seeger, *Z. Naturforsch.* **49A**, 47 (1994).
- ²⁸ K. Konzelmann, G. Majer, M. Notter, and A. Seeger, *Philos. Mag. Lett.* (to be published).
- ²⁹ For the general background of obtaining and analyzing data on defects in metals in high-temperature equilibrium see A. Seeger and H. Mehrer, in *Vacancies and Interstitials in Metals*, edited by A. Seeger, D. Schumacher, W. Schilling, and J. Diehl (North-Holland, Amsterdam, 1970).
- ³⁰ R. Feder and H.P. Charbnau, *Phys. Rev.* **149**, 464 (1966).
- ³¹ M. Ritter, G. Fritsch, and E. Lüscher, *J. Appl. Phys.* **41**, 5071 (1970).
- ³² W. Adlhart, G. Fritsch, and E. Lüscher, *J. Phys. Chem. Solids* **36**, 1405 (1975).
- ³³ D.L. Martin, *Phys. Rev.* **154**, 571 (1967).
- ³⁴ G. Jacucci and R. Taylor, *J. Phys. F* **9**, 1489 (1979).
- ³⁵ R. Bertani, M. Mali, J. Roos, and D. Brinkmann, *J. Phys. Condens. Matter* **2**, 7911 (1990).
- ³⁶ H. Mehrer and N. Stolica, in *Mass and Pressure Dependence of Diffusion in Solid Metals and Alloys*, Landolt-Börnstein, New Series, Vol. 26, edited by H. Mehrer (Springer, Berlin, 1990), Chap. 10.
- ³⁷ H. Mehrer, *J. Nucl. Mater.* **69&70**, 38 (1978).
- ³⁸ D. J. Brinkmann (private communication).
- ³⁹ J.N. Mundy, *Defect and Diffusion Forum* **83**, 1 (1992).
- ⁴⁰ N. V. Doan and Y. Adda, *Philos. Mag. A* **56**, 269 (1987).